



A Semi-empirical Model to Predict the Attached Axisymmetric Shock Shape

A. R. Davari*

Aerospace Division, Department of Engineering, Science and Research Branch, Islamic Azad University, Tehran, Iran

PAPER INFO

Paper history:

Received 21 April 2020

Received in revised form 22 May 2020

Accepted 12 June 2020

Keywords:

Semi Vertex

Mach Wave

Shock Shape

Conical Flow

ABSTRACT

In this work, a simple semi-empirical model is proposed, based on Response Surface Model, RSM, to determine the shape of an attached oblique shock wave emanating from a pointed axisymmetric nose at zero angle of attack. Extensive supersonic visualization images have been compiled from various nose shapes at different Mach numbers, along with some others performed by the author for the present paper. The method is based on the relationship between the body shape and the shock shape. The body shape and the free stream Mach number determine the shape of the oblique shock standing ahead. From the statistical data bank containing the visualization tests and employing the RSM, an analytic relationship has been established between the body and the shock shape. From this relationship, knowing the body shape and the Mach number, one can simply determine the shock shape. The visualization tests performed by the author for some other cases have approved the accuracy of the proposed relationship. However, the approach is restricted to attached shocks emanating from sharp noses at zero angle of attack. Despite the limitations, this relationship can effectively be used in model scale determination for wind tunnel tests to prevent shock reflection from the walls that could lead to erroneous results.

doi: 10.5829/ije.2020.33.08b.23

NOMENCLATURE

<i>M</i>	Free stream Mach number
<i>x</i>	Longitudinal distance along the axis of symmetry from the apex
<i>y_b</i>	The local ordinates of the nose contour
<i>y_s</i>	The local ordinates of the shock
<i>l</i>	The nose length
<i>d</i>	The nose diameter at the base

Greek Symbols

δ	The nose semi vertex angle
μ	Mach wave angle

Subscripts

<i>s</i>	Shock
<i>b</i>	Body/Nose

1. INTRODUCTION

In a supersonic flight, the shock wave emanating from the nose or other components of the aircraft, may impinge somewhere on another solid surface or intersect other waves. Such intersections and interactions are important in the practical design and analysis of the vehicle. This is also the case when a model is to be placed in the wind tunnel test section to avoid any shock intersection with the wall and reflection from it [1-3].

The shape of the attached shock has long been recognized as a subject of remarkable importance, particularly in the solution of interference problems. One

of the primary assumptions to estimate the shock shape of an arbitrary nose shape was to consider it as a straight cone of the same vertex angle as the nose, which is greatly restricted in application. An accurate evaluation of interference requires a careful representation of the curved shock [4].

Some methods have already been proposed to predict the attached shock shape. Among them, the approach based on linear theory, introduced by Whitham [5] has perhaps met with as much success and received as much attention as any others. However, the range of applicability of this method is severely restricted. This method does not give accurate quantitative results when

*Corresponding Author Institutional Email: ardavari@srbiau.ac.ir
(A. R. Davari)

the semi-nose angle is larger than 20° and beyond the Mach number of about 3.0.

Love et al [6] proposed a different approach to obtain the axisymmetric shock shape emanating from a pointed nose. Based on the known shock slope at the apex and that at the end of the nose where the body slope vanishes, he considered an equation for a so-called unspecified shock shape. He suggested that this unspecified shock shape belongs to a circular arc in general. If this arc is put on the given nose contour and adjusted to cover the nose, the unspecified shock and the one correspond to the given nose will be coalesced on each other. This method, despite claims to give good results, is not easy to follow and requires many manual adjustments, which does not grab the interests nowadays.

For calculating shock shape over wide ranges of Mach number and nose shape, the method of characteristics, though being laborious, is still a popular tool. However, in recent years, with the advent of modern processors, the computational methods as well as the experimental surveys are widely used to determine the shock shape and its stand-off distance for the bow and detached shocks [7-10].

Up to now, extensive surveys, mostly numerical, have been performed to study the shock shape, either attached oblique shock or detached one in the form of a bow shock and valuable information have been obtained so far to discover the impact of free stream condition and the body mold line on the shape of the shock wave. However, no attempt has so far been reported in the literature to obtain a neat and easy-to-use analytic relationship between the shock and the body shapes.

The shape of an oblique shock is a key feature to design and determine the scale of the model for supersonic wind tunnel tests. The shock waves emanating from various parts of the model, with an improper scale, could impinge the walls and reflect over the model [11, 12]. This remarkably decreases the accuracy of measurement and the data fidelity. The shock shape is also a major contributor in aerodynamic interference between the components of a supersonic vehicle. The shock-shock, shock-body interactions add lot of complexities to design and analysis of supersonic vehicles [13, 14].

Such applications necessitate accurate shock shape prediction in a minimum time. The numerical calculations to get the shape of the shock for a given flow condition and body shape, is a time-consuming task. Since various conditions have to be examined to get the best results, this would be an iterative process and the numerical calculations cannot be helpful. A rapid engineering, analytic or empirical/semi-empirical relation can be a convenient surrogate tool to determine whether or not, the shock wave impinges to the wind tunnel wall or to another part of the aircraft or to the shock wave emanating from other parts of the vehicle.

Several attempts have already been made to develop an analytical or relationship. The most successful one was proposed by Love [6]. However, he did not offer a ready-to-use and specific relation for any nose shape. He instead, proposed a graphical algorithm in which the user should swing a circular arc along the line normal to the slope of the nose under consideration. This circular arc should be fitted on the front portion of the nose and in this way, a proper scale factor is determined to relate the general shock shape to the specific nose under consideration (Figure 1). The method is cumbersome and hard to use. As stated earlier, it requires many manual adjustments and change of the constants during the process. It soon became obsolete and the researchers kept seeking for proper surrogates.

On the other hand, in recent years the statistical methods using response surface methodology, RSM, has become a popular tool to construct mathematical models based on experimental observations [15-17]. The RSM has provided a promising road for various aerospace applications including the aerodynamic problems. In this methodology, the dependent variable is expressed in the form of a polynomial, in terms of the independent variables engaged in the problem [18]. This process is based on ample experimental observations.

In this paper, a simple semi-empirical model has been proposed, based on RSM methodology, to predict the shock shape on a pointed axisymmetric nose at zero incidence. Several images from various shock visualization methods have been examined and the shock shape for different bodies and different Mach numbers were extracted. With these data, a response surface model was constructed to establish a relationship between the shock shape, as the dependent variable, and the nose geometric parameters and the free stream Mach number as the independent variables.

The proposed regression model was then compared with the data that have not already been used in the regression process. These data were extracted from the Schlieren tests performed by the author and were used to check the model accuracy and validity. The comparisons show a remarkable agreement between the experimental findings, both the data found in the literature and the exclusive ones performed in this paper, and those predicted by the proposed model. The model works for

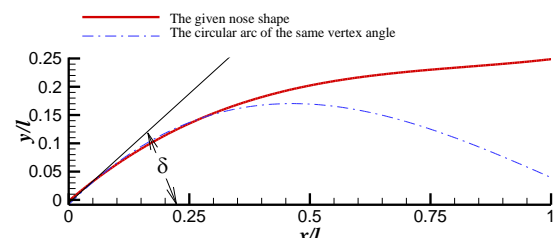


Figure 1. The circular arc fit on the given nose shape

any attached shock ahead of arbitrary axisymmetric pointed bodies of revolution at zero angle of attack. For the case of two-dimensional shock from a wedge, the same approach with a simpler model can be obtained, as well.

2. IDENTIFICATION OF A RESPONSE SURFACE MODEL

The Response Surface Methodology, RSM, encompasses a set of mathematical and statistical methods to model the problems in which a dependent variable is expressed as a function of some independent factors [19].

For m independent variables, x_1, x_2, \dots, x_m , the dependent or response variable, y , can be considered to be an unknown function of the independent variables, i.e. $y = f(x_1, x_2, \dots, x_m)$. For each of N experimental runs carrying out on m design variables and for a single response y , a general form of the regression equation can be considered in the form of Equation (1):

$$y = B_0 + \sum_{i=1}^m B_i x_i + \sum_{i=1}^m B_{ii} x_i^2 + \sum_{i=1}^m B_{iii} x_i^3 + \sum_{i=1}^m \sum_{j \neq i} B_{ij} x_i x_j + \dots + \epsilon \quad (1)$$

where ϵ is the regression error term and the B_{ij} 's are the regression coefficients and are determined by the Least Square method based on several observations of the dependent variable for a given set of the independent parameters [20].

Note that all of the terms in Eq. (1) do not necessarily appear in every problem and some of them according to their functionality and the physical nature of the problem under consideration may be disregarded.

In this paper, the response variables are the terms in the proposed equation for the shock shape and the independent variables are the terms describing the equation of the nose contour as well as the free stream Mach number.

3. THE EXPERIMENTAL DATA COMPENDIUM

Extensive visualization tests have already been performed on various body shapes in supersonic flow to reveal the shock and expansion waves and study their behavior. Some of the clearest ones have been selected from the literature, mostly from Van Dyke's collection [17]. Figure 2 shows these pictures that include different pointed noses at an extensive range of Mach numbers and at zero angle of attack.

In addition to the data bank, shown in Figure 2, which were used to construct a regression model for the shock shape, further Schlieren visualization tests have been performed by the author to check the accuracy of the proposed model. These tests were carried out for various nose shapes at different Mach numbers.

The experiments have been conducted in two supersonic wind tunnels, one having a 60 cm×60 cm test section and the other, which was a small educational tunnel, has a rectangular test section of 2.5 cm×2.8 cm. Figure 3 shows the Schlieren arrangement including the light source, the mirrors, the knife edges and the digital camera recorder for the second tunnel. Shown in Figure 4 are some of the test results.

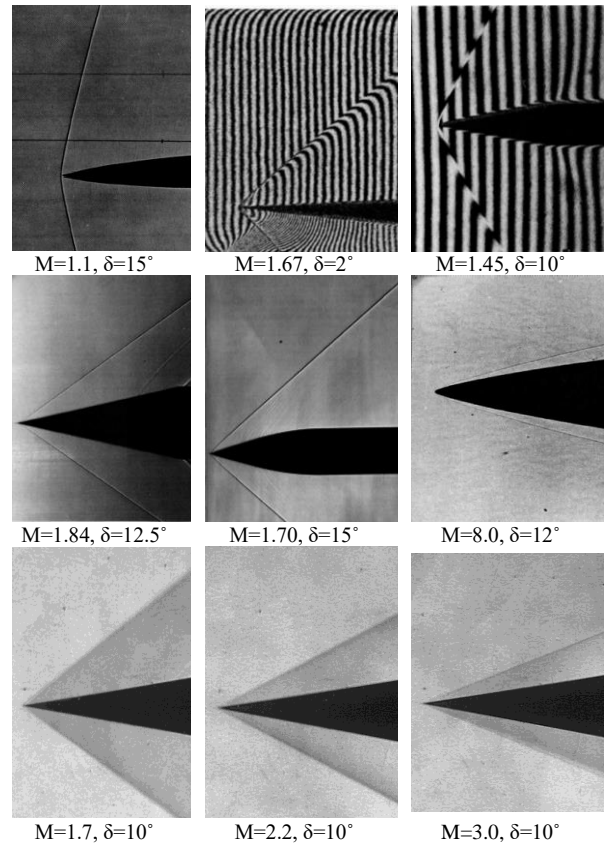


Figure 2. Various attached shocks compiled from the literature [17-19]

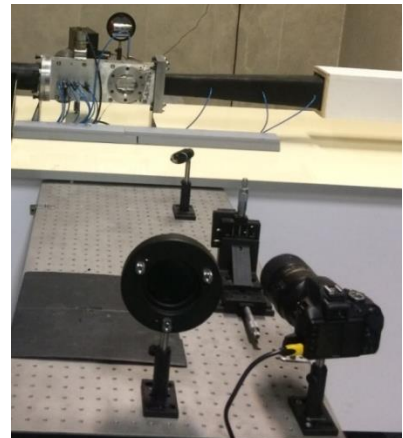


Figure 3. The Schlieren arrangement for the small test section wind tunnel

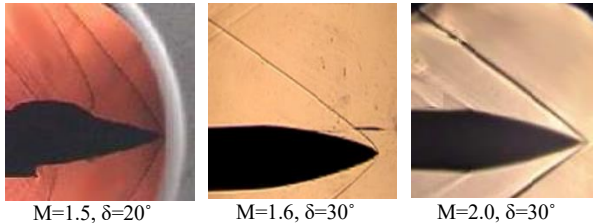


Figure 4. The Schlieren tests performed in the present experiments

The first model is the well-known Standard Dynamics Model, SDM, which is a generic airplane model extensively used to study the dynamic stability behavior and to check the validity of the dynamic test rigs all over the world. The two others are the ogive-cylinder combinations with different nose shapes. The middle nose is a tangent ogive, while the two others are secant.

3. THE SCHILIEREN IMAGE PROCESSING

Picking up the exact points on the shock from the Schlieren images is actually an erroneous task and care must be taken in measuring the shock points. When the image is zoomed-in to pick up the points on the shock, the dark pixels on the shock form discrete saw-tooth cells and cannot be easily distinguished from the background pixels.

To enhance the accuracy of the measurements, an image processing routine was developed using MATLAB®. In the first step, and to simplify the process, the original RGB image, Figure 5(a), was changed to gray scale, Figure 5(b). A histogram plot of the color spectrum from absolute black to absolute white for the image of Figure 5(b) is shown in Figure 5(c). As observed, the intensity peaks are mainly concentrated at two specific regions while the rest of the spectra are nearly empty.

By stretching the color map, the intensity values in grayscale image, Figure 5(b), have covered the entire spectra and were re-scaled in Figure 5(d), such that 1% of data is saturated at low and high intensity regions in Figure 5(b). This increases the contrast of the output image, Figure 5(d). Note that the pixels in the original image have not been displaced by this process, and the shock shape is thus preserved. The improved histogram of the intensities in the spectrum after stretching is shown in Figure 5(e), which approves that the intensities over the gray scale spectra has been stretched and provided a more uniform contrast between the shock and the background pixels. The background color was also removed to get a more distinguished boundary between the shock and the surrounding, Figure 5(f). Finally, using Otsu's method [24], a global threshold was computed that could be used to convert the intensity image to a binary one in which the variance of the black and white pixels is minimized. This can reduce the saw-tooth edges between the pixels and makes them nearly smooth.

The final results would be a clearer boundary between the shock and the environment and is shown in Figure 5(g). The boundary between the dark and the bright zones is actually the outer edge of the shock wave and the points on it were detected and measured with more accuracy. By this method, the shock shape and position have not been changed or displaced, so the shock points recognition have been much easier and more accurate than any classical and conventional methods. The measured quantities from the images were the longitudinal and lateral positions of the points on the nose as well as the ones on the shock all the way from apex to the end of the nose section, along with the nose semi vertex angle, δ . Figure 6 schematically shows the measured parameters.

4. THE REGRESSION MODEL

The shape of a vast range of tangent ogive pointed noses can be expressed in the form of a 4th order polynomial, i.e.

$$y_b = a_1x + a_2x^2 + a_3x^3 + a_4x^4 \quad (2.a)$$

where both x and y_b are normalized by l , and therefore x is between 0 and 1. For non-tangent noses, including the secant types, this approximation still works. Figure 7 shows several tangent, power-law and secant type noses

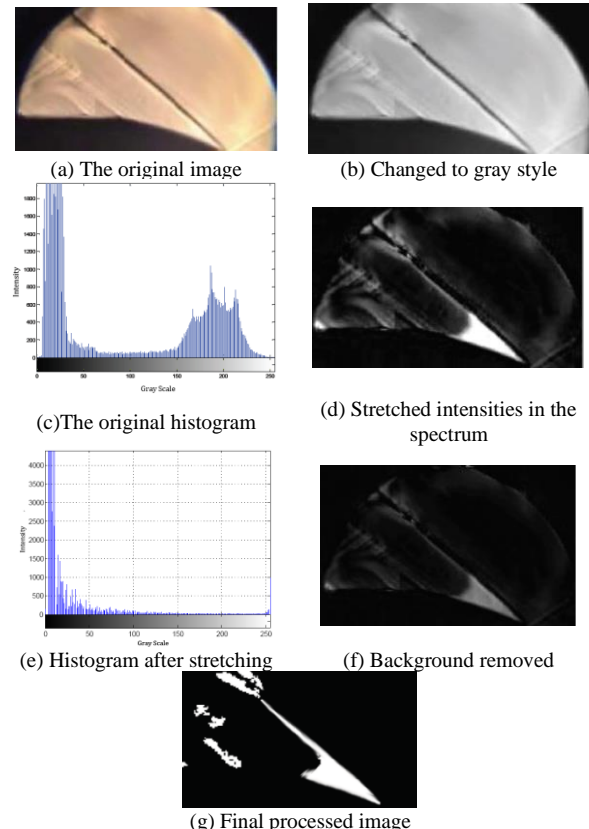


Figure 5. The image processing steps to obtain clear images with a smooth shock boundary

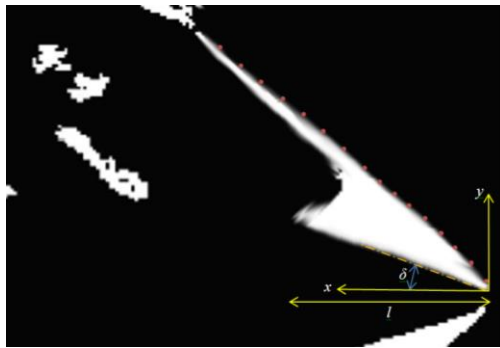


Figure 6. The parameters measured from the processed images

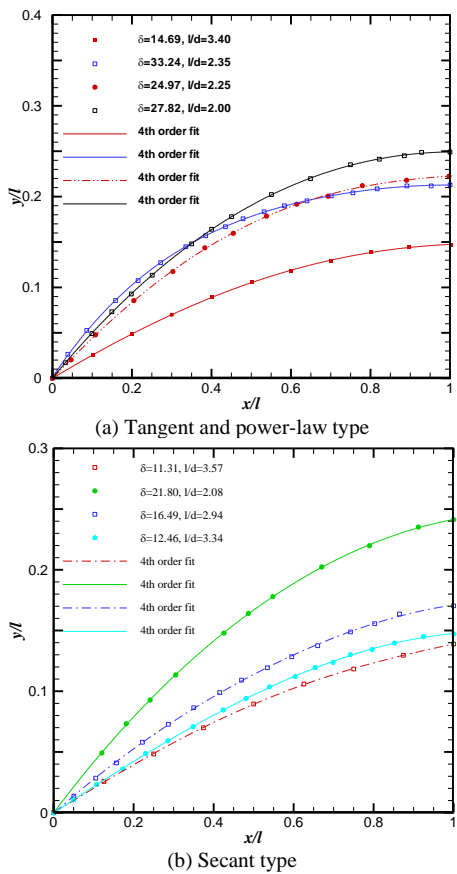


Figure 7. The 4th order polynomial fit on several pointed noses

fitted by a 4th order polynomial, where the markers are the actual points on each nose and the lines of the same color, show the polynomial fit for that nose.

Note that the expansion waves emanating from the front half of the nose usually impinge the nose shock and affect its slope and curvature. After a certain distance from the nose apex, the expansion waves no longer intersect the shock. These stations that are at the rear most of the nose can be deemed to have no effect on shock shape. This has been previously shown by exploiting

method of characteristics on both two-dimensional and axisymmetric pointed bodies [6].

The 4th order polynomial is thus a good approximation for any pointed nose, having a smooth contour, to determine the corresponding shock shape. The shape of the oblique shock emanating from the nose apex would be of the same family of polynomials indicated by Equation (2.a). Evidently, certain relationships must exist between the corresponding coefficients of the two polynomials.

$$y_s = b_1 x + b_2 x^2 + b_3 x^3 + b_4 x^4 \quad (2.b)$$

Again, both x and y_s are normalized by l . First, note that the shock slope at $x=0$ can be considered to be the same as that for an equivalent conical shock angle emanating from a cone of the same semi vertex angle as the body under consideration. At large values of x , i.e. the rear most of the nose, the shock slope reduces to that of the corresponding Mach wave, that is $\arcsin(1/M)$. Therefore:

$$\text{At } x/l=0: dy/dx = \tan \beta$$

$$\text{At } x/l \rightarrow 1: dy/dx = \tan \mu$$

where β is the shock angle and μ the Mach wave angle. Thus, the coefficient b_1 in the shock shape equation must be a function of the body slope, as well as the free stream Mach number. Since the shock slope everywhere decreases with Mach number and increases with the body semi vertex angle, δ , the ratio M/δ plays a decisive role in the shape of the shock.

Note that δ/M is the dominant factor near $x=1$. Since the curvature in the shock shape near $x=0$ is higher than the other longitudinal positions, a third power of a_1 is included to the regression equation for b_1 as well as an interaction term $a_1 a_2$ to match the behaviors at the two limits $x/l=0$ and $x/l=1.0$ and represent a continuous curve. The following functional form can thus be proposed for the constant b_1 in shock equation:

$$b_1 = B_{01} + B_{11} a_1 M/\delta + B_{21} a_1 \delta/M + B_{31} a_1 a_2 + B_{41} a_1^3 \quad (3)$$

The coefficient of the second order term of the shock equation, b_2 , determines the second derivative of the shock equation at the apex. It also depends on M/δ at the front and δ/M at the rear halves of the nose.

This coefficient, b_2 , must also be in accordance with the corresponding value a_2 in the body equation. From the shock shape, it is required for the second derivative in Equation (2) to be always negative. The interaction terms $a_1 a_2$ and $a_3 a_2$ are included to take the dependencies in a_1 and a_3 into account. These terms are necessary to model the impingement of the expansion waves from the nose and the oblique shock originating at the apex. As a consequence, of this impingement, the oblique shock curvature evidently changes. Thus, the regression equation for b_2 may be suggested as:

$$b_2 = B_{02} + B_{12} a_2^2 + B_{22} a_2 M/\delta + B_{32} a_2 \delta/M + B_{42} a_1 a_2 + B_{52} a_3 a_2 \quad (4)$$

Similar regression models have been considered for b_3 and b_4 , knowing the constants a_1 through a_4 from the given nose shape. The third order coefficient for the shock, b_3 , can be modeled to be functions of the products a_3M/δ for the front part and $a_3\delta/M$ for the rear part of the body, along with the interaction terms a_1a_3 and a_1a_2 to adjust the changes in shock slope as the nose local slope changes.

The same arguments work for b_4 which includes the M/δ and M/δ ratios for both near $x=0$ and near $x=1$ respectively, and the interaction terms to express the shock shape as the body slope changes.

$$b_3 = B_{03} + B_{13}a_3 M/\delta + B_{23}a_3\delta/M + B_{33}a_1a_3 + B_{43}a_1a_2 \quad (5)$$

$$b_4 = B_{04} + B_{14}a_1 M/\delta + B_{24}a_1a_4 + B_{34}a_1a_2 + B_{44}a_4\delta/M \quad (6)$$

To make sure that all of the terms added to the response surface model for each coefficient in Equation (3) to (6), were the major contributors to the response variable, the statistical hypothesis test in RSM is performed to determine the p-value [15]. For each term in the regression, the null hypothesis implies that the term under consideration does not have any significant effect on the response variable.

From the Anderson–Darling test [25], if the p-value for that term is greater than a certain pre-defined value, known as the significance level and is usually set to 0.05, the null hypothesis is accepted. This means that the term under consideration does not have any remarkable effect on the coefficients b_1 , b_2 , b_3 or b_4 .

On the other hand, if the p-value is less than the significance level, there would be enough evidence to reject the null hypothesis. The p-values for all of the coefficients were measured to be nearly zero. On this basis, within 95% confidence level, all of the terms used in the regression equation for each coefficient can be considered to have strong impact on the response variables, i.e. b_1 through b_4 .

Each regression equation for b_1 , b_2 , b_3 and b_4 was solved individually using the least square method based on the shock shape measurements already performed for various bodies and the unknown regression constants B_{ij} have been determined.

The regression coefficient, R^2 , in RSM is a measure of the model performance in fitting the data. Theoretically, the closer be R^2 to the unity, the better would be the estimation of regression [25]. The regression coefficient, R^2 , and the adjusted regression coefficient, R_{adj}^2 [25], for each coefficient in Equation (2) have been calculated and shown in Table 1.

Finally, the regression coefficients for Equation (2.b) have been evaluated and are presented in Tables 2-5.

Once the constants b_1 through b_4 are evaluated using the associated regression models, the shock shape is determined from Equation (2.b). This equation holds for any axisymmetric shock on a pointed nose at zero angle of attack.

TABLE 1. The coefficients of regression for each coefficient in the shock shape equation

Coefficient	R^2 (%)	R_{adj}^2 (%)
b_1	99.99	99.97
b_2	99.75	98.50
b_3	98.99	96.96
b_4	99.74	99.21

TABLE 2. The regression constants for b_1

B01	B11	B21	B31	B41
0.748396	-4.50195	0.101269	0.295592	0.933427

TABLE 3. The regression constants for b_2

B02	B12	B22	B32	B42	B52
-0.10824	-19.2161	1.22114	0.21092	-15.2768	-15.2215

TABLE 4. The regression constants for b_3

B03	B13	B23	B33	B43
0.002284	-4.08483	-0.173138	5.44873	-1.47554

TABLE 5. The regression constants for b_4

B04	B14	B24	B34	B44
0.0698898	-2.73123	8.64948	0.346297	-0.280287

To sum up, the procedure followed in this paper to determine the shock shape is elucidated. The problem starts with a given nose at a given Mach number at zero angle of attack. From the geometry of the nose, a 4th order polynomial is fitted on the nose and the coefficients a_1 through a_4 in Equation (2.a) are determined. With these data, the Mach wave angle, μ , and the nose semi vertex angle, δ , can be calculated. Now the shock equation can be determined from Equation (2.b) where the constants b_1 through b_4 are in Equations (4) through (6). The constants in these equations are presented in Tables (2) to (6). The numerical constants have been evaluated from the RSM model, Equation (1), and using several shock shapes obtained from visualization tests.

5. RESULTS AND DISCUSSIONS

Having determined the regression coefficients for the shock shape, Equation (2.b), given a nose shape, the equation of the attached shock can be determined. Various noses at different Mach numbers which have not been used in the regressions to determine B_{ij} , as well as

those exclusively tested in the wind tunnel for the present experiments will be considered in this section to evaluate the performance of the model in Equation (2.b).

The shock shapes ahead of two different noses at a Mach number of $M=1.62$ have been predicted by Equation (2) and compared with the experiment [6]. The prediction accuracy for the nose with $\delta=19.8^\circ$ in Figure 8 is much higher than the other nose shown in Figure 9. This shows that the present approach works better for small nose angles. The agreement between the predicted and measured shock shapes that both the equivalent cone concept at the shock origin and the limit of the shock slope at the end of the nose that have been implemented in Equation (2) worked satisfactorily.

However for $\delta=27.83^\circ$, some small discrepancies are observed between the predicted shock shape and that measured in the experiment. These discrepancies are in the rear half of the nose near the base. From axisymmetric flow theories in supersonic regime, the maximum vertex angle for which, an attached shock is possible at $M=1.62$ is about 30 degrees [26], beyond which the shock will detach the nose and the prediction accuracy decreases.

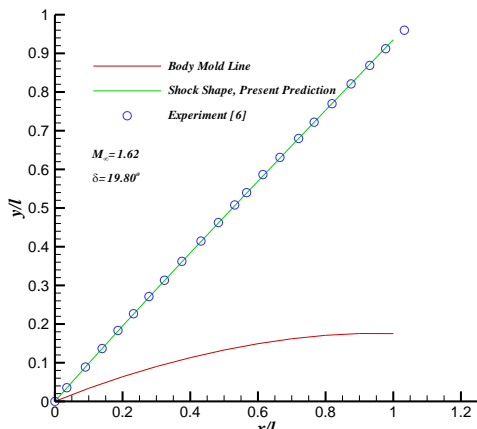


Figure 8. The predicted shock shape for $M=1.62$, $\delta=19.8^\circ$ compared to data of Ref. 6

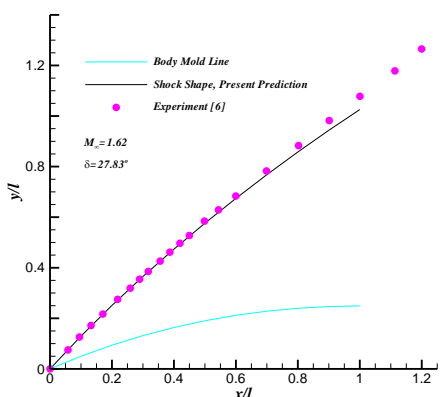


Figure 9. The predicted shock shape for $M=1.62$, $\delta=27.83^\circ$ compared to data of Ref. 6

Similar behavior for another nose with $\delta=30^\circ$ at $M=1.6$ can be observed in Figure 10. The visualization tests for this nose was performed by the author for the present paper, and shows subtle errors in the shock shape predicted by Equation (2) comparing to that measured from the Schlieren tests. For a high supersonic speed of $M=5.05$, Figure 11 shows a good performance for Equation (2) in predicting the shock shape comparing to the experimental data of reference 6. Note that the shock lies closer to the body as the free stream Mach number increases. This makes the shock shape more complicated than the one at smaller Mach numbers and the local slope of the shock would be more sensitive to the nose shape.

Another cases whose Schlieren tests were performed by the author, are shown in Figure 12 for $M=1.5$, $\delta=20^\circ$ and Figure 13 for $M=1.5$, $\delta=20^\circ$. Both noses were secant ogives and one can still observe a remarkable accuracy in shock shape prediction. For the nose in Figure 12, even though the vertex angle is not too large, the nose local slopes are fairly high which adds a lot of complexities to the shock shape. For this reason, some small differences can be seen near the nose base between the predicted and the measured values.

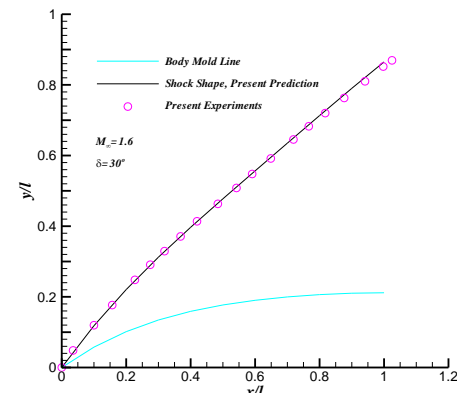


Figure 10. The predicted shock shape for $M=1.6$, $\delta=30^\circ$ compared to the present experiments

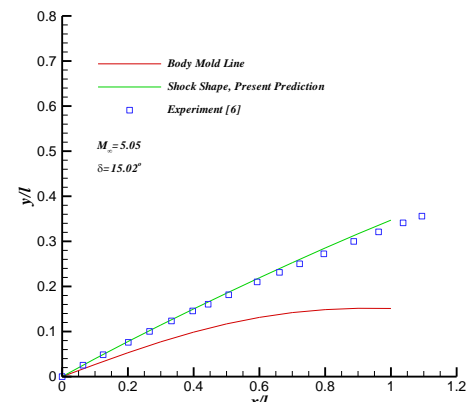


Figure 11. The predicted shock shape for $M=5.05$, $\delta=15.02^\circ$ compared to data of ref. 6

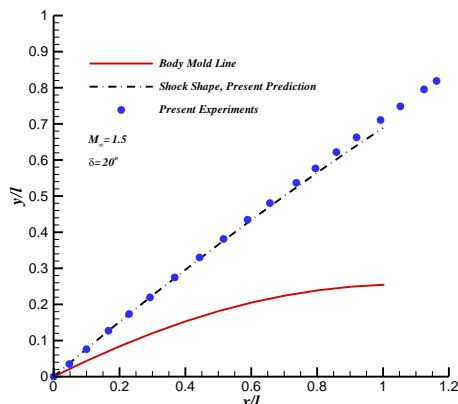


Figure 12. The predicted shock shape for $M=1.5$, $\delta=20^\circ$ compared to the present experiments.

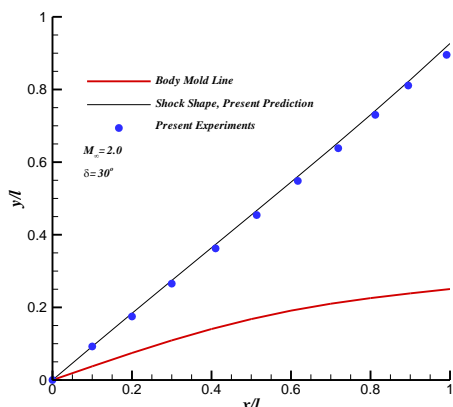


Figure 13. The predicted shock shape for $M=2.0$, $\delta=30^\circ$ compared to the present experiments

6. CONCLUSION

A semi-empirical model has been proposed to determine the shape of the shock wave emanating from a pointed nose, knowing the nose geometric parameters and the free stream Mach number. The method is based on a relationship between the shock shape and the body shape. A series of supersonic flow visualization tests have been compiled and the shock shapes have been correlated to their associated nose shapes. A response surface methodology has been exploited to describe the mathematical model for this relationship. Once the regression coefficients for the model have been determined, it can be used to calculate the shape of the shock, knowing the geometric parameters of the nose. Several Schlieren tests have been performed in this paper to check the validity of the model. The results show a good agreement between the shock shape predicted by this regression model and the ones measured directly from the visualization images for a vast range of nose geometric parameters and free stream Mach numbers. Based on the nature of this model and the supersonic flow properties, the prediction accuracy is likely to slightly

decrease for high Mach numbers where the shock lays closer to the nose surface and at high nose vertex angle where the shock curvature increases and stays away from the nose. The shape of the shock is of great importance when a model of a supersonic vehicle is to be tested in wind tunnel, to avoid shock reflections from the walls.

6. REFERENCES

1. Martínez-Ruiz, D., Huete, C., Sánchez, A.L., and Williams, F.A., "Interaction of Oblique Shocks and Laminar Shear Layers", *AIAA Journal*, Vol. 56, (2018), pp. 1023-1030. DOI: 10.2514/1.J056302.
2. Mason, F. and Kumar, R., "Study of Shock Wave Boundary Layer Interactions on an Axisymmetric Body", AIAA 2019-0342, AIAA Scitech Forum, Shock Boundary Layer Interaction Session, (2019), CA, USA
3. Farahani, M. and Jaber, A., "Experimental Investigation of Shock Waves Formation and Development Process in Transonic Flow", *Scientia Iranica, Transaction B*, Vol. 24, No. 5 (2017), 2457-2465. DOI: 10.24200/sci.2017.4309.
4. Kulkarni, M.D., "Shape Sensitivity for High-speed Flows with Shocks", AIAA 2020-0888, AIAA Scitech Forum, Aerodynamic Shape Optimization Session, (2020), FL, USA
5. Whitham, G.B., "The Flow Pattern of a Supersonic Projectile", *Communications on Pure and Applied Mathematics*, Vol. 5, No. 3, (1920), 301-348. DOI: 10.1002/cpa.3160050305.
6. Love, E.S. and Long, R.H., "A Rapid Method for predicting Attached-Shock Shape", NACA TN-4167, 1957.
7. Martel, J.D., and Jolly, B., "Analytical Shock Standoff and Shape Prediction with Validation for Blunt Face Cylinder", AIAA 2015-0523, AIAA Atmospheric Flight Mechanics Conference, (2015).
8. Sinclair, J. and Cui, X., "A theoretical approximation of the shock standoff distance for supersonic flows around a circular cylinder", *Physics of Fluids*, Vol. 29, (2017), 026102. DOI: 10.1063/1.4975983
9. Hunt, R.L., and Gamba, M., "Shock Train Unsteadiness Characteristics, Oblique-to-Normal Transition, and Three-Dimensional Leading Shock Structure", *AIAA Journal*, Vol. 56, (2018), 1569-1587. DOI: 10.2514/1.J056344
10. Davari, Ali, R., and Soltani, M.R., "On the Relationship between Unsteady Forces and Shock Angles on a Pitching Airplane Model", *Scientia Iranica, Transaction B*, Vol. 17, No. 2, (2010) 102-107. DOI: 10.1063/1.4821520
11. Jin J., Li G., Wei Z., Dong J., Zhang J. "Calibration of the Versatile Platform and the Supersonic Integrated Section" in CAAA. The Proceedings of the 2018 Asia-Pacific International Symposium on Aerospace Technology (2019), Springer, Singapore, Vol. 459. 915-929, DOI: 10.1007/978-981-13-3305-7_72
12. Chernyshev, S.L., Ivanov, A.I., Streletsov, E.V., And Volkova, A.O., "Numerical and Experimental Research of New Methods For Wall Interference Reduction In Wind Tunnels of Transonic and Low Supersonic Velocities", Proceeding of the 7th European Conference on Computational Fluid Dynamics, ECFD 7, (2018), Glasgow, UK
13. Martínez-Ruiz, D., Huete, C., Sánchez, A.L., and Williams, F.A., "Interaction of Oblique Shocks and Laminar Shear Layers," *AIAA Journal*, Vol. 56, (2018), 1023-1030. DOI: 10.2514/1.J056302
14. Mason, F. and Kumar, R., "Study of Shock Wave Boundary Layer Interactions on an Axisymmetric Body," AIAA 2019-0342, AIAA Scitech 2019 Forum, Shock Boundary Layer Interaction Session, (2019), CA, USA, DOI: 10.2514/6.2019-0342

15. Fenrich, R.W., and Alonso, J., "A Comparison of Response Surface Methods for Reliability Analysis using Directional Simulation", AIAA 2018-0437, AIAA Non-Deterministic Approaches Conference, (2018). DOI: 10.1016/S0167-4730(03)00022-5
16. Vasu, A., and Grandhi, R.V., "A Response Surface Model Using the Sorted k-fold Approach", AIAA 2014-1485, 10th AIAA Multidisciplinary Design Optimization Conference, (2014). DOI: 10.2514/1.J052913
17. Kucuk, U.C., "Application of Response Surface Methodology to Optimize Aerodynamic Performance of NACA Inlet," AIAA 2017-4991, 53rd AIAA/SAE/ASEE Joint Propulsion Conference, (2017).
18. Lawson, J., Design and Analysis of Experiments with R, First Edition, CRC Press, (2015).
19. Myers, R.H., and Montgomery, D.C., Response Surface Methodology: Process and Product Optimization Using Designed Experiments, Fourth edition, John Wiley & Sons Inc., (2016). DOI: 10.1080/00224065.2017.11917988
20. Fenrich, R.W., and Alonso, J.J., "A Comparison of Response Surface Methods for Reliability Analysis using Directional Simulation", AIAA 2018-0437, 5th AIAA Non-Deterministic Approaches Conference, (2018), FL, USA. DOI: 10.2514/6.2018-0437
21. Van Dyke, M., An Album of Fluid Motion, The Parabolic Press,, (1982). DOI: 10.1002/aic.690280628
22. D. K. Weimer, C. H. Fletcher, and W. Bleakney, "Transonic Flow in a Shock Tube", *Journal of Applied Physics*, Vol. 20, No. 4, (1949), 418-421. DOI: 10.1063/1.1698393
23. Freeman, N.C., Cash, R.F. and Bedder, D., "An experimental investigation of asymptotic hypersonic flows", *Journal of Fluid Mechanics*, Vol. 18, (1964), 379-384. DOI: 10.1017/S0022112064000271
24. Otsu, N., "A Threshold Selection Method from Gray-Level Histograms," *IEEE Transactions on Systems, Man, and Cybernetics*, Vol. 9, No. 1, (1979), 62-66. DOI: 10.1109/TSMC.1979.4310076
25. Kenett, R.S., Zacks, S., and Amberti, D., Modern Industrial Statistics, Second Edition, John Wiley & Sons Ltd, (2014). DOI: 10.1002/9781118763667
26. Ferreyra, R.T., "Supersonic Cones at Zero Incidence," AIAA 2016-4275, 46th AIAA Fluid Dynamics Conference, (2016). DOI: 10.2514/6.2016-4275

Persian Abstract

چکیده

در این مقاله یک روش نیمه تجربی بر مبنای سطح پاسخ پیشنهاد داده شده است که به کمک آن می‌توان شکل موج ضربه‌ای مایل که از یک دماغه‌ی با تقارن محوری در زاویه‌ی حمله‌ی صفر درجه ایجاد می‌شود را تخمین زد. به این منظور، یک بانک اطلاعاتی گشته‌ده از تصاویر آشکارسازی جریان فراصوتی حول دماغه‌های مختلف در اعداد ماخ متفاوت جمع‌آوری شده و شکل موج ضربه‌ای برای همه‌ی آنها استخراج گردید. همچنین، چندین آزمایش آشکارسازی دیگر با استفاده از امکانات داخلی و در توپل باد فعال موجود در کشور توسط نویسنده انجام گرفته و از نتایج آنها برای بررسی دقت تخمین روش مذکور استفاده شده است. در این روش، ثابت شد که انواع مختلف دماغه‌های با تقارن محوری را می‌توان با یک منحنی درجه‌ی چهار توصیف نمود. بر این اساس، معادله‌ی شکل موج ضربه‌ای نیز یک منحنی درجه‌ی چهار درنظر گرفته شد است که هر یک از ضرایب آن خود تابعی از عدد ماخ جریان و پارامترهای هندسی دماغه می‌باشد. این ضرایب ثابت با استفاده از بانک اطلاعاتی تدوین شده و به کمک روش سطح پاسخ تعیین شده و برای استفاده از روش مذکور، کافیست عدد ماخ جریان و ضرایب معادله‌ی درجه چهار از شکل دماغه مشخص باشند. به کمک اطلاعات مذکور و رابطه‌ی به دست آمده در این مقاله، می‌توان معادله‌ی درجه‌ی چهار از شکل موج ضربه‌ای ایجاد شده را به راحتی تخمین زد. چنین محاسباتی برای به دست آوردن مقیاس مدل مورد آزمایش در توپل باد و به منظور اجتناب از انعکاس شوک از دیواره‌های تونل باد، یک ابزار مهم و کاربردی بوده و نقش مهمی در کاهش خطاهای ناشی از تداخل شوک و دیواره خواهد داشت.
